Calculation of an escapement's profile curve for constructing a mechanical clockwork

$Kai\ \int chmi\,\mathrm{d}t - B\sqrt{auns}$

16 September 2022

Abstract

A specially constructed 3D printable clockwork's escapement is optimized by mathematical means. The result is evaluated by a series of measurements.

Contents

1 Project history

At first glance, the goal of this project may seem very abstract, which is why I would first like to explain how my motivation developed in this direction.
The first suggestion I received for constructing my own mechanical clockwork came from physics class, in which the subject of "oscillations" was dealt with. Mechanical oscillating systems, such as e. g. a piece of mass on a spiral spring, fascinated me so much with their periodic energy conversions that I tried to construct particularly simple ones for 3D printing, and after a few days I found one oscillating in my hands. However, I deemed that something was still missing and slowly I developed my ambition to construct a mechanism that – once wound up – would automatically stimulate the oscillator. And that would be a device that would have the exact properties of a mechanical clockwork.
Ultimately, a small collection of mechanical watches that I own inspired me to start designing the movement. Following that impulse, I had the intention not to simply adopt the mechanical principle of existing escapements, but to come up with my own, which I desired to be particularly simple and minimalistic. It took a few weeks filled with designing, printing, and testing prototypes, and I got my hands on first a satisfyingly oscillating balance wheel, then a gear-driven escapement, which seemed particularly simple to me at the time, and finally I could wind up a completely self-constructed mechanical clockwork depicted in Figure 1 for the first time and it actually ran almost flawlessly. So this seems to be the happy ending of my story about the construction of a mechanical clockwork – one might think.

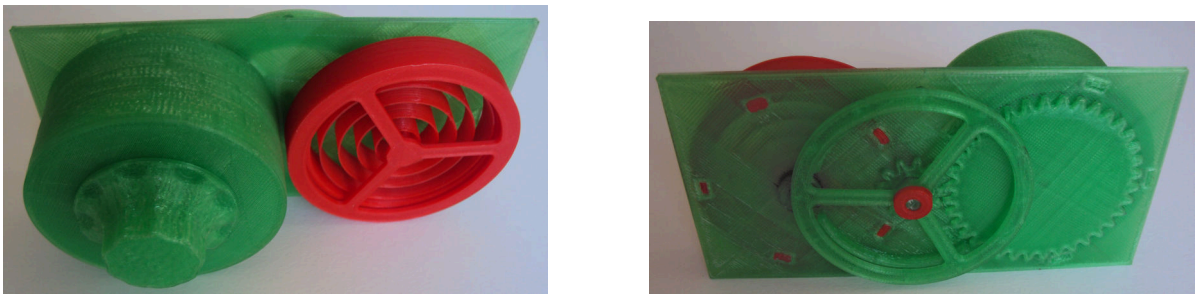

Figure 1: The fully assembled clockwork

In fact, I am still concerned with one detail in my construction, which probably manifests a geometrical problem concerning the escapement of the movement and its profile wheel. As an introduction, I would like to say a few words about the construction and how it works in the next chapter.

2 The clockwork and its mechanical principle

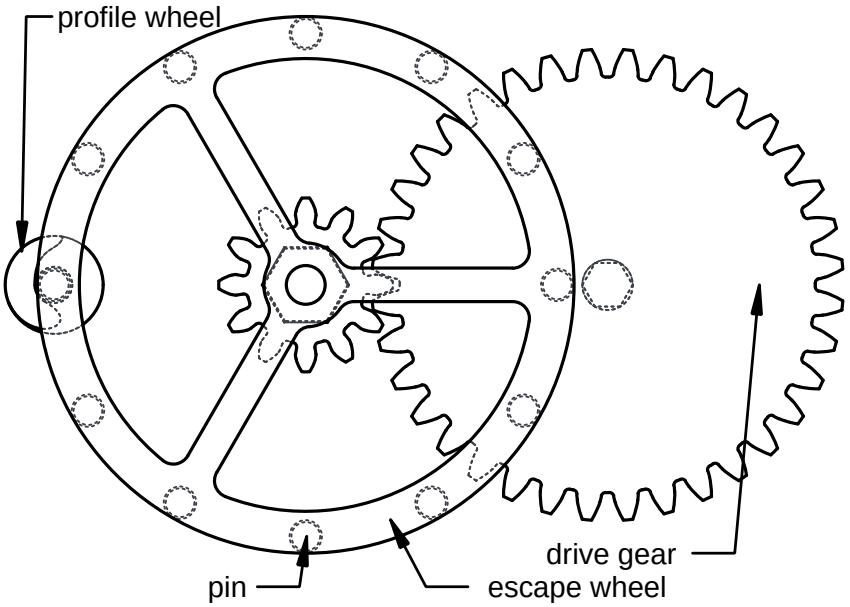

Figure 2: Construction drawing for the most important components of the clockwork

The clockwork can be divided into three main units, which will be described individually in the following subchapters. Figure 2 gives an overview of their mechanical connection to clarify the individual components' interrelations.

2.1 Energy reservoir

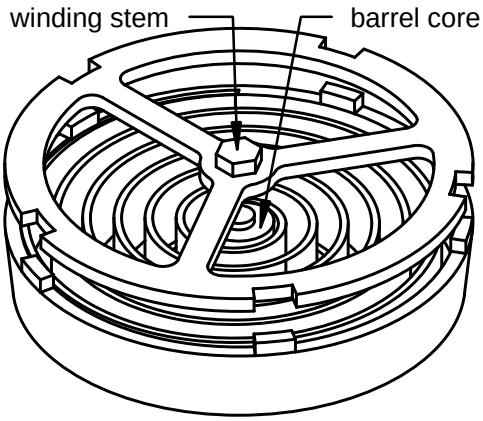

Figure 3: Structure of a barrel: The component with the winding stem is slightly raised for improved visibility. The hexagonal inner profile which is embedded into the bottom of the barrel core is occluded. In the tensioned state, the spring force acts between this barrel core and the winding stem by means of the barrel's outer part. Both hexagonal profiles fit into each other, so that several barrels can be stacked.

In order to excite oscillations against the friction within the system, the clockwork must have a simple energy source. In this case, it consists of a combination of two spiral springs that are tensioned when they are wound. To be more precise, there are two barrels connected in series, the structure of which is shown in Figure 3. One of the spring barrels is fitted with a pawl so that the springs do not relax again immediately after being wound up. This way, the entire spring force acts on the rest of the movement mechanics when the watch is tensioned. The spring of the second barrel is now connected to a large gear wheel, the drive wheel, so that a certain torque is applied to it when it is cocked. In a watch that has clock hands, this gear would also drive their mechanism, but for a pure clockwork movement it is sufficient if it just powers the escapement, which is connected to the drive wheel by a small gear. The escapement's functional description should come last, as it makes a mechanical connection between the mainspring and the balance wheel, which is the main component of the problem this paper deals with.

2.2 Balance wheel

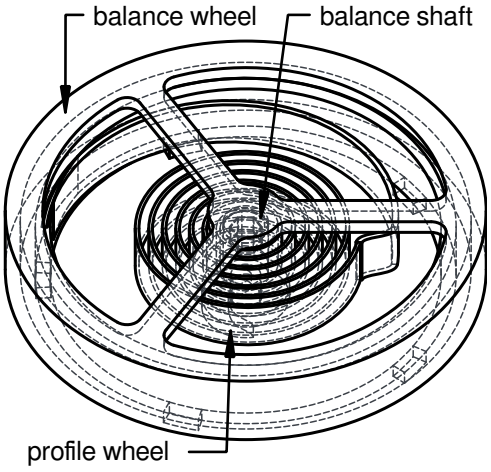

Figure 4: Structure of the balance and its connection to the profile wheel: In order to achieve the greatest possible moment of inertia on the balance wheel with as little material as possible, the mass is distributed as far away from the axis of rotation as possible. One side of the hairspring is connected to the clockwork case on the outside and the other side to the balance shaft and thus also to the profile wheel on the inside.

In a movement, the balance represents a mechanically oscillating system, specifically a torsional oscillator consisting of a rotatably mounted piece of mass, the balance wheel, and a spiral spring attached to it. The rest of the clockwork mechanism is connected via the balance shaft. Figure 4 shows the balance and its direct connection to the profile wheel.
During the oscillation process, the potential energy of the spiral spring and the kinetic energy of the mass, which is connected to its moment of inertia, are periodically converted into one another. One can therefore speak of two alternating phases, which together make up an oscillation cycle. Physical considerations can be used to show that the oscillation cycle has a constant period duration and thus oscillation frequency under ideal circumstances, in which external forces, unfortunately also including the omnipresent friction[1], are absent. This property of almost constant frequency even under realistic circumstances makes the spring-mass system a good approach for a device whose purpose is to measure or keep time.

2.3 Escapement

In mechanical watch movements, escapements help to keep the rotation rate and thus the mechanism's effective rotation speed constant, despite varying torque. This is particularly necessary for watches that are driven by spring force, because their drive springs exert an steadily decreasing torque over time as they relax.
In this paper, a special escapement is to be examined, which – as it turned out after extended research – is also known as the "Tic Tac escapement"[2]. Essentially, it consists of two components. The first is an evenly studded escape wheel, ultimately driven by the mainsprings. The speed-regulating property of the escapement comes about through the interaction of the escapement wheel with the second component, a wheel that has a special profile towards the escapement wheel on one hand and is on the other hand directly connected to the balance via its balance shaft. This profile wheel is traversed by the escapement wheel's pins, which traverse its profile individually and thus mechanically connect the mainsprings to the balance wheel. The special profile determines the force transmission factor[1] as a function of the wheel's rotation angles. If certain conditions are met, the escapement goes through a cycle of four phases, which is repeated with each pin that traverses the profile. In the first phase (Figure 5a) the balance wheel is accelerated in one direction of rotation by the escapement wheel; this is when it is in a driving state. Subsequently, in the second phase (Figure 5b), the escapement wheel is blocked until the balance wheel has reached its resting position after reaching the maximum deflection at which the direction of rotation reverses. Meanwhile, the escapement wheel is in a blocked state. The last two phases (Figure 5c and 5d) are similar to the former ones, with the only

[1]That is – admittedly – a somewhat vague expression. In terms of the following mathematical formulation, it reflects the ratio of torques acting on the escapement wheel and profile wheel.

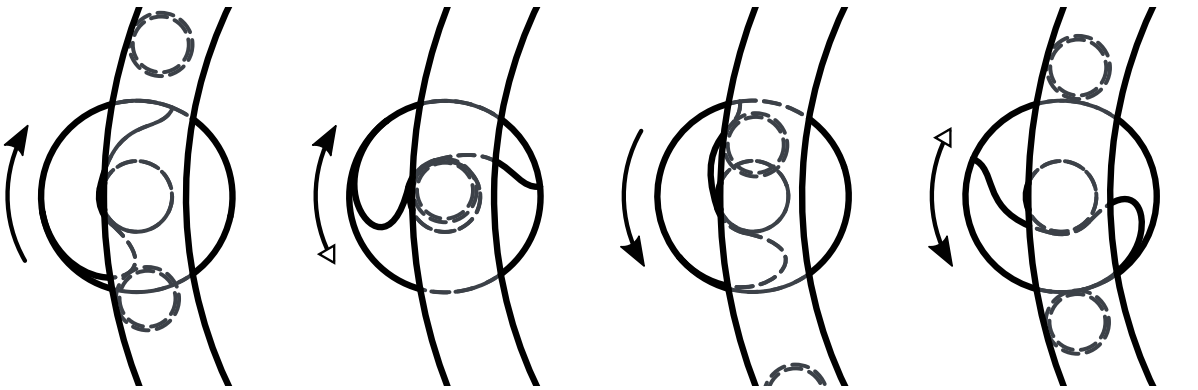

(a) First propulsion phase (b) First blocking phase (c) Second propulsion phase (d) Second blocking phase

Figure 5: Phases of an oscillation cycle: The escapement wheel turns clockwise. Arrows indicate the direction of the profile wheel's rotation, with the white arrow following the black arrow where applicable.

difference being that the balance wheel is accelerated in the opposite direction of rotation. Since the escapement wheel is equipped with 12 pins, it rotates by an angle of $\zeta = \frac{\pi}{6}$ in radians per cycle.
Ideally the reader now has a rough understanding of the presented construction's functional principle, so the next sections can continue dealing with the main problem and the associated mathematical considerations.

3 Main problem

As can be seen from the preceding, the profile of the profile wheel is of crucial importance for this type of escapement. It should therefore be examined which properties an ideal function of the force transmission factor should have as a function of the angles of rotation[2] and by which means the curve of the special profile can be calculated from this function.

3.1 Profile requirements

Before proceeding to the actual goal of calculating the profile curve, a few considerations should be made in preparation to acknowledge which properties of the profile are desirable.
An ideal movement is as stable as possible, i. e. it has a very regular rate and a small beat error. This can only be achieved by reducing distrubances of the balance wheel's oscillating movements as low as possible, which implies minimizing the duration of energy transfer to the balance wheel and keeping energy transfers near its zero crossing.[3]
In addition, it would be desirable for the clockwork to run as long as possible with one winding operation. For this purpose, the friction losses should be kept low and the escapement should be able to work with the widest possible range of torques.

[2]The angles of rotation can also be calculated in a trivial way from the balance wheel's oscillation phase.

4 Various approaches and their results

In order to find the profile curve that satisfies my needs, I considered various approaches and pursued them with more or less success. Before I tackled this problem with mathematical methods, I tried to find a working curve by trial and error to prove the concept of working, printed movement. I set up the first prototypes of the escapement using Bézier curves in FreeCAD[4], my CAD program of choice[5, p. 37, 6, pp. 6–7]. It wasn't until later that I was willing to give this much thought to optimize the profile curve.

4.1 Approach via isogonal trajectories in polar coordinates

Following success with the rather empirical approach, the next challenge is a mathematically based construction, i. e. the profile curve should ideally be calculated unambiguously from comprehensible conditions or at least according to well-defined parameters.
In order to formalize the constellation in which the escapement wheels are located, I first thought it useful to consider the curves and points of the system from a polar coordinate system, the pole of which should be the profile wheel's axis of rotation. Within this setting, a profile curve could be represented as a function of the radius depending on the angle $r(\varphi)$.
Assuming the escape wheel was not supposed to transmit any force to the profile wheel, then the profile curve would match the trajectory of the escape wheel. The key idea was to calculate an isogonal trajectory for this "zero curve", i. e. profile curve with a force transfer factor of zero at every point. This should then have the property of a profile curve in which the trajectory of the escapement wheel's pins always describe the same angle to it. If this is indeed the case, one could introduce another function with which these same angles can be modulated as a function of the wheels' rotation angles. This would essentially achieve the goal of calculating the profile curve according to well-defined parameters.

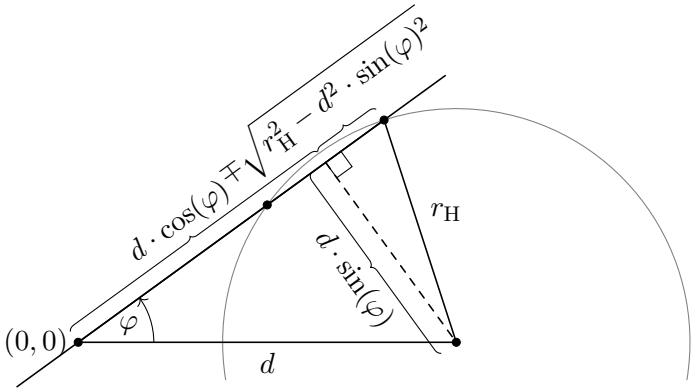

Figure 6: geometry of a shifted circle in polar coordinates

The function equation of the zero curve can be found relatively easily after some geometrical considerations shown in Figure 6:

$$r_0(\varphi) = d\cos(\varphi) \mp \sqrt{r_H^2 - d^2 \sin(\varphi)^2} \tag{1}$$

where r_H is the radius of the escapement wheel and d the center distance between itself and the profile wheel. It should be noted at this point that the positive branch of r_0 is chosen as for the special case $d = r_H$, the negative one always describes the pole i. e. it is zero[3], i. e. the entire domain of r_0 is covered by the positive branch. Figure 7 shows the null curve r_0 with parameters set corresponding to my construction.
In order to calculate the isogonal trajectory to r_0 with an angle α, one would – at least in a

[3]The negative branch of $r_0(\varphi)$ then becomes $r_H \cdot (\cos(\varphi) - \cos(\varphi)) = 0$, while the positive branch becomes $r_H \cdot (\cos(\varphi) + \cos(\varphi)) = 2r_H \cos(\varphi)$.

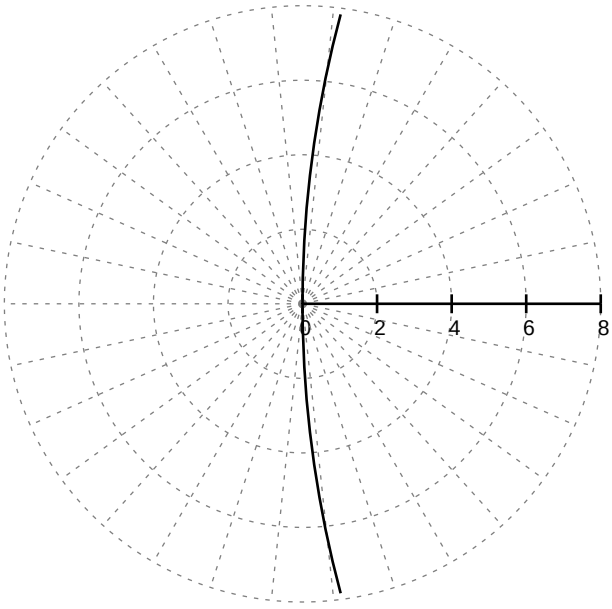

Figure 7: The zero curve given in Equation 1 is chosen with $d = r_\mathrm{H} = 30$, since the profile wheel's center is 30 mm away from that of the escapement wheel and that also is the radius of the circle on which the pin's centers move. The function is shown for $\varphi \in \left[\frac{\pi-\zeta/2}{2}; 2\pi - \frac{\pi-\zeta/2}{2}\right[$, so its curve does not go beyond the profile wheel.

Cartesian coordinate system – directly use the addition theorem for the tangent[4] to enlarge the slopes at each point by that angle. I'm not sure if it is possible do the same with polar functions, but I tried it anyway, hoping that differentiation and integration in the polar coordinate system would have the properties I expected them to have.
For the further procedure one must first calculate the slope angles as a function of φ, which is the arctangent of the derivative:

$$\beta(\varphi) = \arctan(r_0') = \arctan\left(d\cos(\varphi) - \frac{d^2\cos(\varphi)\sin(\varphi)}{\sqrt{r_\mathrm{H}^2 - d^2\cos(\varphi)^2}}\right) \tag{2}$$

Now β and the constant angle α are substituted into the addition theorem followed by integration, whose result should be a function that has the given angle difference to the zero curve at every point:

$$r(\varphi) = \int_0^\varphi \frac{\tan(\alpha) + r_0'(\psi)}{1 - \tan(\alpha)\cdot r_0'(\psi)}\,\mathrm{d}\psi \tag{3}$$

It turns out that in the rarest cases an antiderivative for isogonal trajectories can be found analytically[5], which is why I used the open-source mathematics program wxMaxima[9] to numerically calculate the resulting profile curve and by means of a little trick[6]it is possible to make it plot the resulting function.
I had curves calculated for different angles, but the plot shown in Figure 8 reveals at first glance that this is not the curve I'm looking for, which is why I didn't pursue further thoughts on this approach for the time being. Presumably the failure is due to the fact that my dubious assumption that my approach using isogonal trajectories make sense to polar functions is wrong. For the results of this approach, I will therefore save myself from printing a corresponding profile wheel and testing it on the movement due to theoretically justified concerns.

[4] $\tan(\alpha+\beta) = \frac{\tan(\alpha)+\tan(\beta)}{1-\tan(\alpha)\tan(\beta)}$ [7]

[5] In this case I first tried it by hand, then with GeoGebra[8] and wxMaxima, both failing, sometimes even with program crashes.

[6] For some reason wxMaxima does not allow plotting numerically integrated functions directly. But you can wrap the operation of numerical integration in a lambda expression that passes the values to the plotter. It may sound absurd, but it actually works.

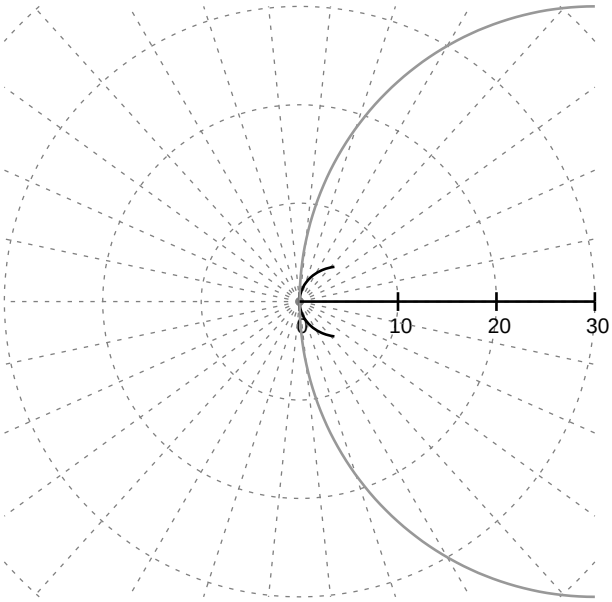

Figure 8: Zero curve (grey) and its numerically calculated isogonal trajectory (black) with an angle difference of $-10°$ in the polar coordinate system: It probably does not deliver the desired result, because the tangents of the two curves do not always have the same angular difference at intersections with the same rays originating from the pole. Especially the points near the pole are emphasized for clarification.

4.2 Via torque ratios using geometry and analysis

When I had a lot of free time again, I tried the problem again. In this approach, the wheel constellation is first formalized as a composed rotation in a Cartesian coordinate system, which is attached the profile wheel, as depicted in Figure 9. It makes sense that the origin of the coordinate system is also the center of rotation of the first rotation, which is described by the angle α by which the mechanism is inclined around the profile wheel. The mechanism inclined in this way contains the escapement wheel, whose angle of rotation is denoted by β.

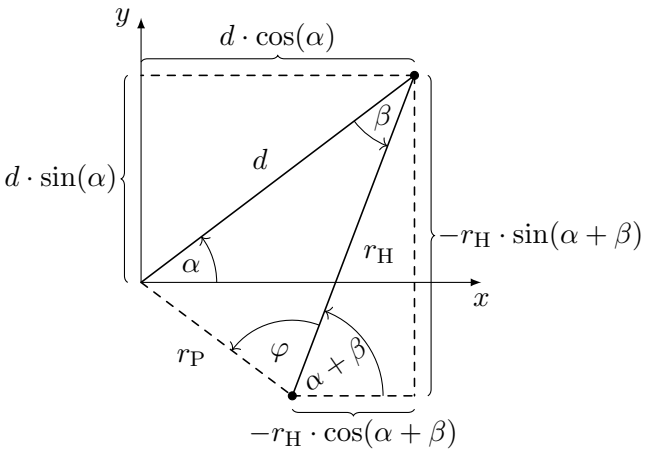

Figure 9: Angles and distances of the new view: The dashed line r_P corresponds to the profile's radius at the point of contact between the profile and a pin on the escapement wheel. The point of contact depends on the angles α and β.

Now in this coordinate system, a parametric curve describing a pin's trajectory when viewed from the profile wheel and depending on the rotation angle of the escapement wheel is defined:

$$\vec{p}(\beta) = \begin{pmatrix} d\cos(\alpha(\beta)) - r_\mathrm{H}\cos(\alpha(\beta)+\beta) \\ d\sin(\alpha(\beta)) - r_\mathrm{H}\sin(\alpha(\beta)+\beta) \end{pmatrix} : \beta \in \left[-\frac{\Delta\beta}{2}; \frac{\Delta\beta}{2}\right[\tag{4}$$

d then is the distance between the escapement wheel's and the profile wheel's center, r_H the escapement wheel's radius, $\alpha(\beta)$ is a function that represents the reverse[7] of the profile wheel's

[7] A positive direction of the mechanism's rotation *inside* coordinate system is a negative direction of rotation *of* the coordinate system and thus of the profile wheel.

rotation angle and $\Delta\beta = \zeta$ stands for the angle between two pins on the escapement wheel, which means that the view applies for exactly one oscillation cycle, i. e. two beats.

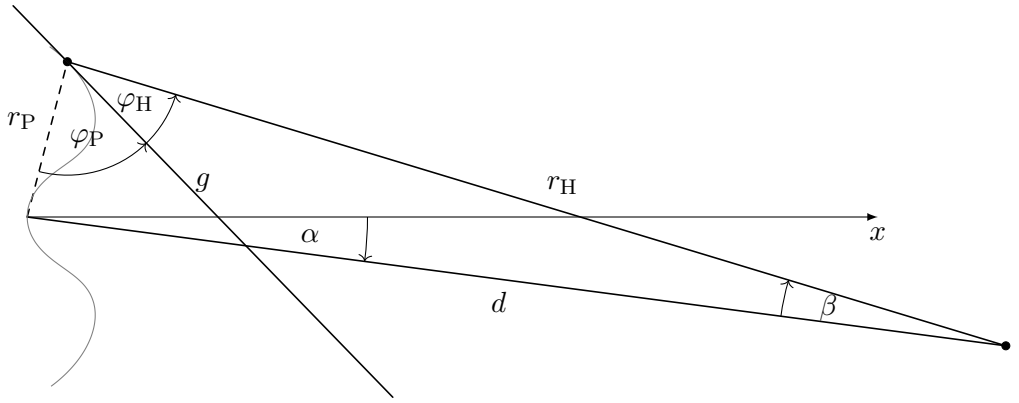

Figure 10: Force decomposition at the curve tangent: The tangential force from the escapement wheel acting counter-clockwise on the profile wheel is distributed at the profile tangent g, so that it is forced to turn in the same direction, i. e. α decreases.

This form proves to be an extremely useful tool for setting other parameters of the curve, such as the force transmission factor. To do this, it is necessary to determine the angle between the profile's tangent shown in Figure 10 and the segments r_H and r_P connecting the point of contact with their centers of rotation, respectively, at the point of contact between pin and profile wheel. These angles φ_H and φ_P are ultimately required for a force decomposition such that the ratio of the escapement wheel's and profile wheel's torques for a given function $\alpha(\beta)$ can be calculated or an α with given torque ratios can be found. The slope of the tangent at a certain angle of rotation β is the quotient of x- and y-component's derivatives, by means of the intelligent arctangent[8]:

$$p'_y(\beta) = d \cdot \alpha'(\beta) \cdot \cos(\alpha(\beta)) - r_\mathrm{H} \cdot (\alpha'(\beta) + 1) \cdot \cos(\alpha(\beta) + \beta) \tag{5}$$

$$p'_x(\beta) = -d \cdot \alpha'(\beta) \cdot \sin(\alpha(\beta)) + r_\mathrm{H} \cdot (\alpha'(\beta) + 1) \cdot \sin(\alpha(\beta) + \beta) \tag{6}$$

$$\delta_\mathrm{T}(\beta) = \operatorname{arctan2}\left(\frac{p'_y(\beta)}{p'_x(\beta)}\right) = \operatorname{arctan2}\left(\frac{d \cdot \alpha'(\beta) \cdot \cos(\alpha(\beta)) - r_\mathrm{H} \cdot (\alpha'(\beta) + 1) \cdot \cos(\alpha(\beta) + \beta)}{-d \cdot \alpha'(\beta) \cdot \sin(\alpha(\beta)) + r_\mathrm{H} \cdot (\alpha'(\beta) + 1) \cdot \sin(\alpha(\beta) + \beta)}\right) \tag{7}$$

It should be noted that the angle is measured relative to the x-axis of the coordinate system. The line r_H connected to the escapement wheel's center of rotation has an angle that can be found directly using Figure 9: $\delta_\mathrm{H} = \alpha + \beta$, so that the angle between r_H and the tangent g is given by:

$$\varphi_\mathrm{H} = \delta_\mathrm{T} - \delta_\mathrm{H} = \delta_\mathrm{T} - \alpha - \beta \tag{8}$$

For the other line segment r_P connected to the profile wheel, the law of sines leads to the angle between the segment and g if its length is known. This is given by the Pythagorean theorem:

$$r_\mathrm{P} = \sqrt{r_\mathrm{H}^2 \sin(\beta)^2 + (d - r_\mathrm{H} \cos(\beta))^2} \tag{9}$$

[8]The intelligent arctangent is characterized by the fact that it finds the correct angle from the numerator and denominator of the "fraction" (these are then the arguments), which is not just an element of $]-\pi;\pi[$. An example: $\operatorname{arctan2}\left(\frac{1}{-1}\right) = 3\pi/4$, while $\arctan(-1) = -\pi/4$.

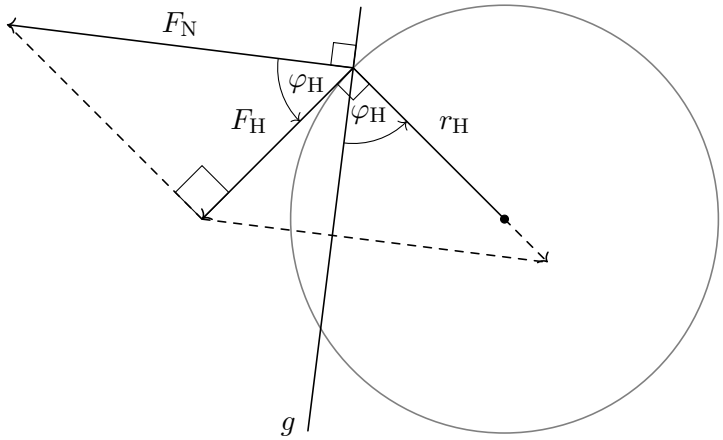

Figure 11: Force distribution on the straight line g, which is tangent to the profile curve, on the escapement wheel

And finally, the law of sines can be used as the unknown angle φ_P determined by the angle $\varphi = \varphi_\mathrm{P} + \varphi_\mathrm{H}$ opposing d:

$$\frac{\sin(\varphi_\mathrm{P} + \varphi_\mathrm{H})}{d} = \frac{\sin(\beta)}{r_\mathrm{P}} \tag{10}$$

$$\varphi_\mathrm{P} = \arcsin\left(\frac{d}{r_\mathrm{P}}\sin(\beta)\right) - \varphi_\mathrm{H} \tag{11}$$

$$= \arcsin\left(\frac{d\sin(\beta)}{\sqrt{r_\mathrm{H}^2\sin(\beta)^2 + (d - r_\mathrm{H}\cos(\beta))^2}}\right) - \delta_\mathrm{T} + \alpha + \beta \tag{12}$$

From the angles that are now known, one can finally calculate the force transmission factor, from which the ratio of the torques follows directly. In this escapement, the force F_H acting tangential to the track, i. e. acting perpendicular to the radius of the escapement wheel, is first broken down into a component F_N that is perpendicular to the profile curve tangent and thus parallel to its normal. Using the forces diagram in Figure 11, one can see that these two forces fulfill the relationship

$$F_\mathrm{H} = F_\mathrm{N}\cos(\varphi_\mathrm{H}) \tag{13}$$

, if $\varphi_\mathrm{H} = \delta_\mathrm{T} - \delta_\mathrm{H}$ denotes the angle between escapement wheel radius and profile curve tangent. After this intermediate step, the sought force, i. e. the force acting tangentially to the profile wheel's circular path, can be determined. This decomposition is similar to the first in the intermediate step, except that this time the force along the normal is known and the tangential force is unknown. In other words: the same formula applies to the second decomposition, where $F_\mathrm{N} = F_\mathrm{N}$, $F_\mathrm{H} = F_\mathrm{P}$ and $\varphi_\mathrm{H} = \varphi_\mathrm{P}$, so that after substitution the following relation holds:

$$F_\mathrm{P} = F_\mathrm{N}\cos(\varphi_\mathrm{P}) \tag{14}$$

Now two equations can be divided and the formula for the force transmission factor at given angles arises:

$$\frac{F_\mathrm{H}}{F_\mathrm{P}} = \frac{\cos(\varphi_\mathrm{H})}{\cos(\varphi_\mathrm{P})} \tag{15}$$

The final step leading to the relationship of torques is to rearrange the definition according to force and substituting:

$$F = \frac{M}{r} \qquad \Rightarrow \qquad \frac{\frac{M_\mathrm{H}}{r_\mathrm{H}}}{\frac{M_\mathrm{P}}{r_\mathrm{P}}} = \frac{\cos(\varphi_\mathrm{H})}{\cos(\varphi_\mathrm{P})} \qquad \Rightarrow \qquad \frac{M_\mathrm{H}}{M_\mathrm{P}} = \frac{r_\mathrm{H}\cos(\varphi_\mathrm{H})}{r_\mathrm{P}\cos(\varphi_\mathrm{P})} \tag{16}$$

Now it is only a matter of substituting both angles, which results in a function of the torque ratio as a function of β and, above all, the function α:

$$\eta(\beta) = \frac{M_\mathrm{H}}{M_\mathrm{P}} = \frac{r_\mathrm{H}}{r_\mathrm{P}} \cdot \frac{\cos(\delta_\mathrm{T} - \delta_\mathrm{H})}{\cos\left(\arcsin\left(\frac{d}{r_\mathrm{P}}\sin(\beta)\right) - \delta_\mathrm{T} + \delta_\mathrm{H}\right)} \quad \left| \begin{array}{l} \text{Recursively substituting } r_\mathrm{P} \text{ and all } \delta; \\ \cos(x) = \cos(-x) \end{array} \right. \tag{17}$$

$$= \frac{r_\mathrm{H}}{\sqrt{r_\mathrm{H}^2 \sin(\beta)^2 + (d - r_\mathrm{H}\cos(\beta))^2}} \cdot \frac{\cos\left(\arctan2\left(\frac{d\cdot\alpha'\cdot\cos(\alpha) - r_\mathrm{H}\cdot(\alpha'+1)\cdot\cos(\alpha+\beta)}{-d\cdot\alpha'\cdot\sin(\alpha) + r_\mathrm{H}\cdot(\alpha'+1)\cdot\sin(\alpha+\beta)}\right) - \alpha - \beta\right)}{\cos\left(\arctan2\left(\frac{d\cdot\alpha'\cdot\cos(\alpha) - r_\mathrm{H}\cdot(\alpha'+1)\cdot\cos(\alpha+\beta)}{-d\cdot\alpha'\cdot\sin(\alpha) + r_\mathrm{H}\cdot(\alpha'+1)\cdot\sin(\alpha+\beta)}\right) - \arcsin\left(\frac{d\sin(\beta)}{\sqrt{r_\mathrm{H}^2\sin(\beta)^2 + (d - r_\mathrm{H}\cos(\beta))^2}}\right) - \alpha - \beta\right)} \tag{18}$$

As the attentive reader has certainly noticed after a few algebraic transformations in his head, $\eta(\beta) = -\alpha'(\beta)$ actually holds. If this relationship doesn't seem obvious to you, please reach for pen and paper to prove it as a little exercise.
The "little exercise" was, of course, a gross understatement for what it takes to get there; I therefore apologize for the joke. Before it even occurred to me to test this assumption, I had GeoGebra plot $\alpha(\beta)$ and $\eta(\beta)$, whereupon I noticed that the latter bears a suspicious similarity to the derivative of the former: And indeed, subtracting $-\alpha'$ gives zero for all β in the plot area! Motivated by this remarkable property of the torque ratio function, I grabbed pen and paper myself (first A4, then due to lack of space A3) to prove my assumption using various trigonomic identities. Due to the fact that the last steps consist of transforming extremely long fractions, which go beyond the space and scope of this main part, I will limit myself here to the final result. The complete derivation in Appendix A shows that the complicated term of $\eta(\beta)$ reduces completely except for

$$\eta(\beta) = -\alpha'(\beta) \tag{19}$$

, which confirms my initial suspicion. From this knowledge, the surprisingly trivial[9] conclusion that the momentary torque ratio at the escapement wheel's rotation angle β is given exactly by the derivative of the function $-\alpha(\beta)$, which is the profile wheel's angle of rotation in relation to that of the escapement wheel[10], can be drawn.

4.3 Confirmation of the result using physics

The escapement presented is a form of mechanical energy transfer that obeys the law of conservation of energy. So it can be assumed that all the turning work done by the escapement wheel also appears on the profile wheel. Therefore, as is usual with many other problems in physics, the fact that energy is neither supplied from outside the system nor escaped from it can be used to analyze the system.
In general, energy is defined as force over distance, i. e.

$$E = \int F(s)\,\mathrm{d}s \tag{20}$$

In the special case of the escapement, turning work of the escapement wheel is converted into turning work of the profile wheel. Combined with the definitions of torque $M = F \cdot r$ and angle $\varphi = \frac{s}{r}$, this results in:

$$E_\mathrm{D} = \int \frac{M(s)}{r}\,\mathrm{d}s = \int M\left(\frac{s}{r}\right)\,\mathrm{d}\frac{s}{r} = \int M(\varphi)\,\mathrm{d}\varphi \tag{21}$$

[9] The same follows from more simple considerations, taking into account the conservation of energy, as will be shown later.

[10] $\alpha(\beta)$ itself gives the angle of rotation of the movement to the profile wheel, so $-\alpha(\beta)$, i. e. with a negative sign, the angle of rotation of the profile wheel to the clockwork. This matter is – as is so often the case with mathematical models – a question of the choice of the coordinate system.

, i. e. torque over angle of rotation.
The first thing to consider is the energy ΔE_H emitted by the escapement wheel when rotating from any starting angle σ to the end angle β:

$$\Delta E_\mathrm{H} = \int_\sigma^\beta M_\mathrm{H}(\varphi)\,\mathrm{d}\varphi \tag{22}$$

The energy absorbed by the profile wheel is ΔE_P when it has rotated from its starting angle $-\alpha(\sigma)$ to the ending angle $-\alpha(\beta)$[11]:

$$\Delta E_\mathrm{P} = \int_{-\alpha(\sigma)}^{-\alpha(\beta)} M_\mathrm{P}(\varphi)\,\mathrm{d}\varphi \tag{23}$$

This equals to – one may believe the law of conservation of energy – the energy emitted by the escapement wheel, i. e. $\Delta E_\mathrm{H} = \Delta E_\mathrm{P}$:

$$\int_\sigma^\beta M_\mathrm{H}(\varphi)\,\mathrm{d}\varphi = \int_{-\alpha(\sigma)}^{-\alpha(\beta)} M_\mathrm{P}(\varphi)\,\mathrm{d}\varphi \qquad \Big|\ \frac{\mathrm{d}}{\mathrm{d}\beta} \tag{24}$$

Because this expression is an equation, the same operation can be performed on both sides without affecting the validity of the statement. Here, deriving both sides with respect to β leads to the goal. Since the energy integral concerning the escapement wheel is bounded by the function α, the chain rule may be applied:

$$M_\mathrm{H}(\beta) = -M_\mathrm{P}(-\alpha(\beta)) \cdot \alpha'(\beta) \qquad |: M_\mathrm{P} \tag{25}$$

$$\frac{M_\mathrm{H}}{M_\mathrm{P}} = \eta(\beta) = -\alpha'(\beta) \tag{26}$$

, which confirms the result of the last approach: The instantaneous torque ratio of the escapement wheel to the profile wheel at the angle of rotation β is given by the derivative of the angle of rotation function $-\alpha(\beta)$. A profile curve that has a specific torque ratio at a rotation angle β can now be found by integrating the torque ratio function $\eta(\beta)$, which first leads to a corresponding rotation angle function α:

$$\eta(\beta) = -\alpha'(\beta) \tag{27}$$

$$\Rightarrow -\int_0^\beta \eta(b)\,\mathrm{d}b = \alpha(\beta) \tag{28}$$

This may be substituted into the parametric curve p defined by Equation 4 to get:

$$\vec{p}_\eta(\beta) = \begin{pmatrix} d\cos(-\int_0^\beta \eta(b)\,\mathrm{d}b) - r_\mathrm{H}\cos(\beta - \int_0^\beta \eta(b)\,\mathrm{d}b) \\ d\sin(-\int_0^\beta \eta(b)\,\mathrm{d}b) - r_\mathrm{H}\sin(\beta - \int_0^\beta \eta(b)\,\mathrm{d}b) \end{pmatrix} : \beta \in \left[-\frac{\Delta\beta}{2}; \frac{\Delta\beta}{2}\right[\tag{29}$$

With this result, the problem is actually good as solved – one just has to define a function η that meets the requirements, i. e. that i. a. has a reasonable slope near $-\frac{\Delta\beta}{2}$ and zero. However, before the curve that was eventually calculated can be applied to a real profile wheel, one more small detail must be taken into account, which is no less important though: Up to now, the models describing the escapement mechanism have assumed escape wheel pins to be mathematical points. In fact, however, it has a finitely small radius, namely one of 2 mm, not taking into account tolerances in the manufacturing process. In my case – it's an FDM 3D printer – 0.15 mm have proven successful.

[11] As α describes the clockwork's angle of rotation around the profile wheel in relation to the escapement wheel's angle of rotation, the starting and ending angles of the profile wheel must be $-\alpha$.

5 Application of the calculated curve to a real profile wheel using parallel curves

It turned out that the curve calculated by the mathematical model cannot be applied directly to a real profile wheel. A new curve would be desirable, the points of which are "shifted" in one direction compared to the old curve, without the tangent angles changing: For each β, δ_T on the old curve should be equal to the tangent angle which occurs at the circular[12] escape wheel pins' point of contact with the curve.
The new curve must therefore have a tangent parallel to the old curve's tangent for each β, the perpendicular distance of which corresponds to the escapement wheel pin radius. Such a tangent can be calculated from parametric curves by calculating the tangent and then forming the perpendicular vector scaled to the desired distance.

Tangent vector of a parametric curve $\vec{f}(t) = \begin{pmatrix} x(t) \\ y(t) \end{pmatrix}$:

$$\dot{\vec{f}} = \begin{pmatrix} \dot{x} \\ \dot{y} \end{pmatrix} \tag{30}$$

perpendicular:

$$\dot{\vec{f}}_\perp = \begin{pmatrix} -\dot{y} \\ \dot{x} \end{pmatrix} \tag{31}$$

normalized and scaled by distance a:

$$\vec{v}_a = \frac{\dot{\vec{f}}_\perp}{\left\| \dot{\vec{f}}_\perp \right\|} \cdot a \tag{32}$$

each point of $\vec{f}$ shifted by $\vec{v}_a$:

$$\vec{f}_a(t) = \vec{f}(t) + \vec{v}_a \tag{33}$$

$$\Leftrightarrow \vec{f}_a(t) = \begin{pmatrix} x(t) - \frac{\dot{y}}{\sqrt{\dot{x}^2+\dot{y}^2}} \cdot a \\ y(t) + \frac{\dot{x}}{\sqrt{\dot{x}^2+\dot{y}^2}} \cdot a \end{pmatrix} \tag{34}$$

During extended research for this paper, it turned out that such curves – as their main property already suggests – are called parallel curves[10].
The fact that these, together with round pins, are mostly equivalent to the mathematical model of the punctiform pin with regard to the torque ratio function η despite a change in the point of contact can be explained most easily by the fact that parallel curves of the profile curve do not cause any change in the path of the journal relative to the profile wheel. That means they do not change $\alpha(\beta)$ either, so $-\alpha'(\beta)$ also stays the same. As the physical approach also confirms independently of the escapement geometry, this is exactly $\eta(\beta)$, which is also parallel curve invariant.
Now one last problem to be treated theoretically remains open, which first is visualized in Figure 12. The peculiarity lies in the fact that the curve intersects itself, which may not appear to be a problem at first: After all, the designer is free to choose only the points before and after the intersection. However, the path of movement of the escapement wheel pin's center would then differ from the intended path. This would result in the real profile wheel deviating greatly from the mathematical model, i. e. $\eta(\beta)$ no longer applies to all β on the real profile wheel, which is why such curves should be avoided. This deviation is indicated by the dashed arc in the figure.

[12] The escape wheel pivots are actually frustoconical rather than circular because this reduces friction by minimizing the contact area. However, in the two-dimensional projection, which is entirely sufficient for calculating the curve, the escapement wheel pivots are circular.

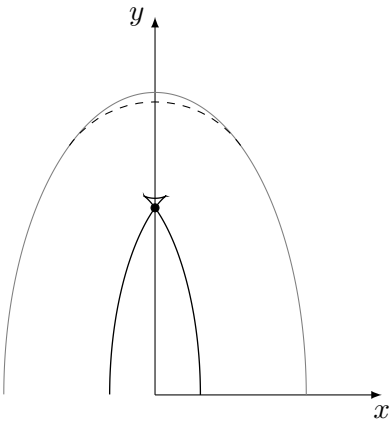

Figure 12: External elliptical curve and an associated parallel curve, where singularities occur due to strong curvature and large distances. In this example, they manifest near the y-axis. If the curve is nevertheless used on a profile wheel, the trajectory of the pin deviates because it rolls off circularly at the curve tip shown as a point.

The fact that singularities occur when a certain maximum of curvature or distance is exceeded raises the question of the qualitative determination of this maximum: Under exactly what circumstances do discontinuities occur in the parallel curve?
To answer this question, it makes sense to think about special cases.
If one looks at a circle function with a certain radius and its parallel curve, you will notice that there is a distance a, so that all points of this circular function are mapped onto a single one. If one further increases the distance, a circle forms again, but it is "inverted" and drawn in the opposite direction to the original circle function, because its points are opposite when viewed from the center. This observation can be transferred to other continuous functions: If one approximates each point of the function by a circle, i. e. its curvature is determined, the direction of the drawing changes abruptly at the point under consideration if the parallel curve distance a falls below the initial curve's curvature radius, and a singularity manifests itself in such a change in direction. This means that such singularities, which are undesirable in practice, occur precisely when the initial curve is curved in the direction of the parallel curve and its radius of curvature is less than the distance between the parallel curves.
This condition can now be checked for mathematically by calculating the radius of curvature of the initial curve. The definition of curvature can be derived from that of the radius of a circle. This is given by the quotient of the total angle in radians[13] and the arc length of the circle. For sectors, the following applies in general:

$$r = \frac{l}{\alpha} = \frac{\mathrm{d}s}{\mathrm{d}\theta} \tag{35}$$

Here, l denotes the arc length and α the sector angle. The same applies to infinitesimal arc lengths $\mathrm{d}s$ and angles $\mathrm{d}\theta$.
Finally, one can apply this equation to functions by determining the change in length and angle at a point in the function. The change in arc length can be easily calculated using the arc length integral:

$$s = \int \sqrt{\dot{x}^2 + \dot{y}^2}\,\mathrm{d}t \tag{36}$$

$$\frac{\mathrm{d}s}{\mathrm{d}t} = \left(\int \sqrt{\dot{x}^2 + \dot{y}^2}\,\mathrm{d}t\right)' = \sqrt{\dot{x}^2 + \dot{y}^2} \tag{37}$$

The arctangent of the tangent angle can be used to find the change in angle:

$$\frac{\mathrm{d}\theta}{\mathrm{d}t} = \left(\arctan\left(\frac{\dot{y}}{\dot{x}}\right)\right)' = \frac{\left(\frac{\dot{y}}{\dot{x}}\right)' \cdot \dot{x}^2}{\dot{x}^2 + \dot{y}^2} = \frac{\dot{x}\ddot{y} - \dot{y}\ddot{x}}{\dot{x}^2 + \dot{y}^2} \tag{38}$$

[13] or the arc length of the unit circle

Substituted into Equation 35:

$$r(t) = \frac{\frac{\mathrm{d}s}{\cancel{\mathrm{d}t}}}{\frac{\mathrm{d}\theta}{\cancel{\mathrm{d}t}}} = \frac{\sqrt{\dot{x}^2 + \dot{y}^2}^3}{\dot{x}\ddot{y} - \dot{y}\ddot{x}} \tag{39}$$

This is the parametric function's radius of curvature as a function of the parameter t, which only leaves one with the task of examining maxima and minima of this function in the given interval and, if necessary, correcting the output curve so that the radii of curvature are below the parallel curve distance.

6 Measurement series to evaluate the calculated curve's performance

In order to check whether the mathematically optimized profile curves have better properties than empirically determined ones, it makes sense – precisely because the movement is completely 3D printable – to produce profile wheels with curves to be compared and to carry out a series of measurements.

6.1 Procedure for recording the series of measurements

Following the selection of suitable test candidates, a special procedure generates measurement data that is used to characterize the clockwork's rate: The ticking of the clock can be used as an indicator for the beginning of blocking phases, because this begins with an escapement wheel pin being stopped abruptly. The said noise arises, which can then be recorded by microphone.
In practical terms, this means: One draws the smartphone, winds up the movement[14] and starts recording. As soon as it stops moving, the series of measurements is complete and the recording stops. I set the initial state of the clockwork in such a way that the first click in the recording occurred during the transition from the escapement into the second blocking phase (Figure 5d)[15].
An audio file is now available that only contains a click sound at the beginning of each blocking phase and can be statistically evaluated using analysis tools, including Audacity[11].
Even if the procedure for recording the series of measurements sounds uncomplicated in itself, in practice there are difficulties: it is possible that the clockwork runs well with a certain orientation in space, despite the profile wheel remaining unchanged, but after a slight change in orientation no oscillation arises at all. The problem is the friction of the moving parts inside the clockwork, which depends on many factors. Depending on how the movement is held, there is more or less friction at different points in different states of the mechanism, presumably due to gravity. As a result, the experiment cannot be reproduced very well. When measuring, I had to empirically determine the optimal orientation of the movement in space.

6.2 Evaluation of the data

The arithmetic mean and the absolute mean deviation as well as the relative mean deviation can be calculated from the beat durations. These values are listed in Table 1 in order to compare the performance of the empirical approach's profile wheels with the mathematically calculated ones.
The first thing to notice is that the average beat durations are different; the calculated profile wheel has a balance oscillation of lower frequency. This alone indicates that the escapement with empirical profile wheel forces a balance oscillation frequency too high due to excessive force, or that the escapement with calculated profile wheel forces a balance oscillation frequency too low due to excessive friction; at least one profile wheel causes the balance wheel to oscillate at a

[14] The movement is wound up the same amount for each series of measurements.

[15] The duration of the first beat is therefore the time interval of the escapement's transitioning from the second blocking phase into the first.

Table 1: statistical evaluation of the measurement data

E = empirical approach; M = mathematical approach

	1. beat duration		2. beat duration		period (both beat durations)	
	E	M	E	M	E	M
average	0.24 s	0.28 s	0.26 s	0.31 s	0.51 s	0.60 s
mean deviation	0.02 s	0.02 s	0.03 s	0.02 s	0.03 s	0.02 s
relative deviation	6.87 %	5.43 %	10.60 %	5.20 %	6.17 %	4.09 %

frequency that is significantly different from its natural frequency.
The fact that the (relative) mean deviation of the calculated profile wheel is smaller suggests that the calculated profile wheel provides a more regular beat rate, so it has already made the hoped-for improvement in this respect. The most important findings from the extended data analysis in Appendix B are that using the calculated profile wheel results in a longer, more regular and less error-prone operation of the movement than the empirically determined profile wheel, which disturbs the balance wheel's oscillations more, so that the oscillation frequency is significantly higher than the natural frequency of the balance wheel, but the oscillation is sustained over a greater span of forces.

7 Outlook

The last approach in conjunction with parallel curves, is at least a theoretically satisfactory solution to the curve calculation problem. The result also turns out to be satisfactory in practice, as the series of measurements can confirm that the calculated curve ensures a clockwork's rate more regular; for further details on the series of measurements see also [6, pp. 12–15].
However, a theoretical aspect of this project is still unclear: The original torque ratio function only corresponds exactly to the derivative of $-\alpha$ if the parameters d and r_{H} take special value ranges. It is therefore apparently contradictory that the function turns out to be independent of the two parameters after simplification. According to my current state of knowledge, this circumstance is related to the fact that the trigonometric inverse functions, especially the arcsine that occurs with the law of sines, actually have several solutions and the standard solutions do not necessarily correspond to the correct angles within the value ranges mentioned. However, while transforming, such detail is lost because I had considered inverse functions of functions to cancel; though for example, $\arcsin(\sin(x))$ is not always equal to x.

8 Acknowledgement

At this point I would like to thank my tutor and mathematics teacher Benjamin Stelter and my seminar lecturer Prof. Dr. Harald Löwe, who supported me in the implementation of the project and motivated me to write the article published in Mathematikinformation. In particular, I owe Mr. Löwe the certainty that the physical confirmation is formally proper.
Valuable comments and discussions from and with Prof. Dr. Bernd Burghardt have helped me to make the mathematical notation more comprehensible at various points in this paper, for which I would like to express my thanks as well.
Thanks to the company IGUS, which specializes in polymers that can be subjected to high mechanical stresses, and which was kind enough to provide me with a roll of their TRIBOFILAMENT, I could carry out the remaining tests.

References

[1] Wikipedia. *Torsionspendel — Wikipedia, Die freie Enzyklopädie*. 2020. URL: https://de.wikipedia.org/w/index.php?title=Torsionspendel&oldid=197287922#Physikalische_Beschreibung.

[2] Pieces of Time. *Rare English Tic Tac Escapement Watch*. URL: https://www.antique-watch.com/product-35-w10085.html?Page=product&URLName=35-w10085.

[3] Wikipedia. *Abfall (Uhr) — Wikipedia, Die freie Enzyklopädie*. 2020. URL: https://de.wikipedia.org/w/index.php?title=Abfall_(Uhr)&oldid=200545181.

[4] Jürgen Riegel. *FreeCAD: An open-source parametric 3D CAD modeler*. URL: https://www.freecadweb.org.

[5] Kai Schmidt-Brauns. "Überlegungen zur Berechnung der Profilkurve für die Hemmung eines mechanischen Uhrwerks". In: *Mathematikinformation* 73 (2020). URL: http://www.mathematikinformation.info/.

[6] Kai Schmidt-Brauns. *Konstruktion und mathematische Optimierung eines vollständig 3D-gedruckten Uhrwerkes*. Jugend forscht Regionalwettbewerb Braunschweig – Technik. 2021.

[7] Wikipedia. *Formelsammlung Trigonometrie — Wikipedia, Die freie Enzyklopädie*. 2020. URL: https://de.wikipedia.org/w/index.php?title=Formelsammlung_Trigonometrie&oldid=196652004#Additionstheoreme.

[8] IGI. *GeoGebra*. 2020. URL: https://www.geogebra.org/.

[9] wxMaxima developers. *wxMaxima*. URL: https://wxmaxima-developers.github.io/wxmaxima/.

[10] Wikipedia. *Parallelkurve — Wikipedia, Die freie Enzyklopädie*. 2020. URL: https://de.wikipedia.org/w/index.php?title=Parallelkurve&oldid=197583077.

[11] Audacity Team. *Audacity®: Free Audio Editor and Recorder [Computer application]*. Audacity® software is copyright © 1999-2021 Audacity Team. The name Audacity® is a registered trademark. 2020. URL: https://audacityteam.org/.

Appendix A Complete derivation

The addition theorems of the sine and cosine functions were of particular importance for the simplification of the long expression. First, a small collection of formulae that proved to be helpful for deriving the result:

$$\sin(-x) = -\sin(x); \qquad \cos(-x) = \cos(x) \tag{40}$$

$$\sin(x+y) = \sin(x)\cos(y) + \sin(y)\cos(x) \tag{41}$$

$$\cos(x+y) = \cos(x)\cos(y) - \sin(y)\sin(x) \tag{42}$$

$$\sin(x) = \pm\sqrt{1-\cos(x)^2}; \qquad \cos(x) = \pm\sqrt{1-\sin(x)^2} \tag{43}$$

$$\sin\left(\operatorname{arctan2}\left(\frac{y}{x}\right)\right) = \operatorname{sgn}(x)\frac{y/x}{\sqrt{(y/x)^2+1}} \tag{44}$$

$$\cos\left(\operatorname{arctan2}\left(\frac{y}{x}\right)\right) = \operatorname{sgn}(x)\frac{1}{\sqrt{(y/x)^2+1}} \tag{45}$$

$$(x+y)^2 = x^2+y^2+2xy; \qquad (x-y)^2 = x^2+y^2-2xy \tag{46}$$

To save space, the following definition is given beforehand: $q = \frac{p'_y}{p'_x}$. Starting from Equation 17 you can proceed as follows:

$$\eta = \frac{r_\mathrm{H}}{r_\mathrm{P}} \cdot \frac{\cos(\delta_\mathrm{T} - \delta_\mathrm{H})}{\cos\left(\arcsin\left(\frac{d}{r_\mathrm{P}}\sin(\beta)\right) - \delta_\mathrm{T} + \delta_\mathrm{H}\right)}$$

$$= \frac{r_\mathrm{H}}{r_\mathrm{P}} \cdot \frac{\cos(\delta_\mathrm{T} - \delta_\mathrm{H})}{\cos\left(\delta_\mathrm{T} - \left(\underbrace{\arcsin\left(\frac{d}{r_\mathrm{P}}\sin(\beta)\right) + \delta_\mathrm{H}}_{\delta_\mathrm{P}}\right)\right)} \quad \text{| 42, 40}$$

$$= \frac{r_\mathrm{H}}{r_\mathrm{P}} \cdot \frac{\cos(\delta_\mathrm{T})\cos(\delta_\mathrm{H}) + \sin(\delta_\mathrm{H})\sin(\delta_\mathrm{T})}{\cos(\delta_\mathrm{T})\cos(\delta_\mathrm{P}) + \sin(\delta_\mathrm{P})\sin(\delta_\mathrm{T})} \quad \text{| 45, 44}$$

$$= \frac{r_\mathrm{H}}{r_\mathrm{P}} \cdot \frac{\operatorname{sgn}(p'_x)\sqrt{q^2+1}^{-1}}{\operatorname{sgn}(p'_x)\sqrt{q^2+1}^{-1}} \cdot \frac{\cos(\delta_\mathrm{H}) + \sin(\delta_\mathrm{H}) \cdot q}{\cos(\delta_\mathrm{P}) + \sin(\delta_\mathrm{P}) \cdot q}$$

$$= \frac{r_\mathrm{H}}{r_\mathrm{P}} \cdot \frac{\cos(\delta_\mathrm{H}) + q\sin(\delta_\mathrm{H})}{\cos\left(\arcsin\left(\frac{d}{r_\mathrm{P}}\sin(\beta)\right) + \delta_\mathrm{H}\right) + q\sin(\delta_\mathrm{P})} \quad \text{| 42, simplify}$$

$$= \frac{r_\mathrm{H}}{r_\mathrm{P}} \cdot \frac{\cos(\delta_\mathrm{H}) + q\sin(\delta_\mathrm{H})}{\cos\left(\arcsin\left(\frac{d}{r_\mathrm{P}}\sin(\beta)\right)\right)\cos(\delta_\mathrm{H}) - \frac{d}{r_\mathrm{P}}\sin(\beta)\sin(\delta_\mathrm{H}) + q\sin(\delta_\mathrm{P})}$$

| 43, simplify

$$= \frac{r_\mathrm{H}}{r_\mathrm{P}} \cdot \frac{\cos(\delta_\mathrm{H}) + q\sin(\delta_\mathrm{H})}{\sqrt{1 - \left(\frac{d}{r_\mathrm{P}}\sin(\beta)\right)^2} \cdot \cos(\delta_\mathrm{H}) - \frac{d}{r_\mathrm{P}}\sin(\beta)\sin(\delta_\mathrm{H}) + q\sin(\delta_\mathrm{P})} \quad \text{| analogously for } \sin(\delta_\mathrm{P})$$

$$= \frac{r_\mathrm{H}}{r_\mathrm{P}} \cdot \frac{\cos(\delta_\mathrm{H}) + q\sin(\delta_\mathrm{H})}{\sqrt{1 - \left(\frac{d}{r_\mathrm{P}}\sin(\beta)\right)^2} \cdot (\cos(\delta_\mathrm{H}) + q\sin(\delta_\mathrm{H})) + \frac{d}{r_\mathrm{P}}\sin(\beta) \cdot (q\cos(\delta_\mathrm{H}) - \sin(\delta_\mathrm{H}))}$$

| extract r_P from root

$$= \frac{r_\mathrm{H}}{\cancel{r_\mathrm{P}}} \cdot \frac{\cos(\delta_\mathrm{H}) + q\sin(\delta_\mathrm{H})}{\underbrace{\sqrt{\frac{r_\mathrm{P}^2 - d^2\sin(\beta)^2}{\cancel{r_\mathrm{P}^2}}}}_{w} \cdot (\cos(\delta_\mathrm{H}) + q\sin(\delta_\mathrm{H})) + \frac{d}{\cancel{r_\mathrm{P}}}\sin(\beta) \cdot (q\cos(\delta_\mathrm{H}) - \sin(\delta_\mathrm{H}))}$$

$$w = \sqrt{r_\mathrm{H}^2\sin(\beta)^2 + (d - r_\mathrm{H}\cos(\beta))^2 - d^2\sin(\beta)^2} \quad \text{| 43}$$

$$= \sqrt{r_\mathrm{H}^2 \cancel{- r_\mathrm{H}^2\cos(\beta)^2} \cancel{+ d^2} \cancel{+ r_\mathrm{H}^2\cos(\beta)^2} - 2 \cdot d \cdot r_\mathrm{H}\cos(\beta) \cancel{- d^2} + d^2\cos(\beta)^2}$$

| 46

$$= \sqrt{(r_\mathrm{H} - d\cos(\beta))^2} = r_\mathrm{H} - d\cos(\beta)$$

$$\eta = \frac{r_\mathrm{H} \cdot (\cos(\delta_\mathrm{H}) + q\sin(\delta_\mathrm{H}))}{(r_\mathrm{H} - d\cos(\beta)) \cdot (\cos(\delta_\mathrm{H}) + q\sin(\delta_\mathrm{H})) + d\sin(\beta) \cdot (q\cos(\delta_\mathrm{H}) - \sin(\delta_\mathrm{H}))}$$

| factor q out

$$= \frac{r_\mathrm{H} \cdot (q\sin(\delta_\mathrm{H}) + \cos(\delta_\mathrm{H}))}{\begin{array}{l} q \cdot ((r_\mathrm{H} - d\cos(\beta)) \cdot \sin(\delta_\mathrm{H}) + d\sin(\beta)\cos(\delta_\mathrm{H})) \\ \quad + (r_\mathrm{H} - d\cos(\beta)) \cdot \cos(\delta_\mathrm{H}) - d\sin(\beta)\sin(\delta_\mathrm{H}) \end{array}}$$

| expand $(r_\mathrm{H} - d\cos(\beta))$

$$= \frac{r_\mathrm{H} \cdot (q\sin(\delta_\mathrm{H}) + \cos(\delta_\mathrm{H}))}{\begin{array}{l} q \cdot (r_\mathrm{H}\sin(\delta_\mathrm{H}) - d\cos(\beta)\sin(\delta_\mathrm{H}) + d\sin(\beta)\cos(\delta_\mathrm{H})) \\ \quad + r_\mathrm{H}\cos(\delta_\mathrm{H}) - d\cos(\beta)\cos(\delta_\mathrm{H}) - d\sin(\beta)\sin(\delta_\mathrm{H}) \end{array}} \quad \text{| 41, 42; } \delta_\mathrm{H} = \alpha + \beta$$

$$= \frac{r_\mathrm{H} \cdot (q\sin(\delta_\mathrm{H}) + \cos(\delta_\mathrm{H}))}{q \cdot (r_\mathrm{H}\sin(\delta_\mathrm{H}) - d\sin(\alpha)) + r_\mathrm{H}\cos(\delta_\mathrm{H}) - d\cos(\alpha)} = \frac{N}{D}$$

| substitute q into numerator and directly expand by p'_x

$$N = \frac{r_\mathrm{H}}{p'_x} \cdot ((d \cdot \alpha' \cdot \cos(\alpha) \cancel{- r_\mathrm{H} \cdot (\alpha' + 1) \cdot \cos(\delta_\mathrm{H}))} \cdot \sin(\delta_\mathrm{H})$$

$$
\begin{aligned}
&\quad + (-d \cdot \alpha' \cdot \sin(\alpha) + r_\mathrm{H} \cdot \cancel{(\alpha' + 1) \cdot \sin(\delta_\mathrm{H})}) \cdot \cos(\delta_\mathrm{H})) && \mid \text{factor out } d \cdot \alpha' \\
&= \frac{r_\mathrm{H}}{p'_x} \cdot (d \cdot \alpha' \cdot (\cos(\alpha) \sin(\delta_\mathrm{H}) - \sin(\alpha) \cos(\delta_\mathrm{H}))) && \mid 41;\ \delta_\mathrm{H} = \alpha + \beta \\
&= \frac{r_\mathrm{H}}{p'_x} \cdot d \cdot \alpha' \cdot \sin(\beta)
\end{aligned}
$$

$$
\eta = \frac{r_\mathrm{H} \cdot d \cdot \alpha' \cdot \sin(\beta)}{p'_x \cdot (q \cdot (r_\mathrm{H} \sin(\delta_\mathrm{H}) - d \sin(\alpha)) + r_\mathrm{H} \cos(\delta_\mathrm{H}) - d \cos(\alpha))} = \frac{N}{D}
$$

| substitute q into numerator and multiply by p'_x consequently

$$
\begin{aligned}
D = {} & (d \cdot \alpha' \cdot \cos(\alpha) - r_\mathrm{H} \cdot (\alpha' + 1) \cdot \cos(\delta_\mathrm{H})) \cdot (r_\mathrm{H} \sin(\delta_\mathrm{H}) - d \sin(\alpha)) \\
& + (-d \cdot \alpha' \cdot \sin(\alpha) + r_\mathrm{H} \cdot (\alpha' + 1) \cdot \sin(\delta_\mathrm{H})) \cdot (r_\mathrm{H} \cos(\delta_\mathrm{H}) - d \cos(\alpha)) \\
& && \mid \text{factor } \alpha' \text{ out} \\
= {} & \alpha' \cdot (\cancel{d \cos(\alpha) \cdot r_\mathrm{H} \sin(\delta_\mathrm{H})} \cancel{- d \cos(\alpha) \cdot d \sin(\alpha)} \\
& \cancel{- r_\mathrm{H} \cos(\delta_\mathrm{H}) \cdot r_\mathrm{H} \sin(\delta_\mathrm{H})} \cancel{+ r_\mathrm{H} \cos(\delta_\mathrm{H}) \cdot d \sin(\alpha)} \\
& \cancel{- d \sin(\alpha) \cdot r_\mathrm{H} \cos(\delta_\mathrm{H})} \cancel{+ d \sin(\alpha) \cdot d \cos(\alpha)} \\
& \cancel{+ r_\mathrm{H} \sin(\delta_\mathrm{H}) \cdot r_\mathrm{H} \cos(\delta_\mathrm{H})} \cancel{- r_\mathrm{H} \sin(\delta_\mathrm{H}) \cdot d \cos(\alpha))} \\
& \cancel{- r_\mathrm{H} \cos(\delta_\mathrm{H}) \cdot r_\mathrm{H} \sin(\delta_\mathrm{H})} + r_\mathrm{H} \cos(\delta_\mathrm{H}) \cdot d \sin(\alpha) \\
& \cancel{+ r_\mathrm{H} \sin(\delta_\mathrm{H}) \cdot r_\mathrm{H} \cos(\delta_\mathrm{H})} - r_\mathrm{H} \sin(\delta_\mathrm{H}) \cdot d \cos(\alpha) && \mid 41 \\
= {} & -r_\mathrm{H} \cdot d \sin(\beta) && \mid \text{substitute } D \text{ back into } \eta
\end{aligned}
$$

$$
\eta = \frac{\cancel{r_\mathrm{H} \cdot d} \cdot \alpha' \cdot \cancel{\sin(\beta)}}{\cancel{-r_\mathrm{H} \cdot d} \cdot \cancel{\sin(\beta)}} = -\alpha'
$$

Appendix B Extended data analysis

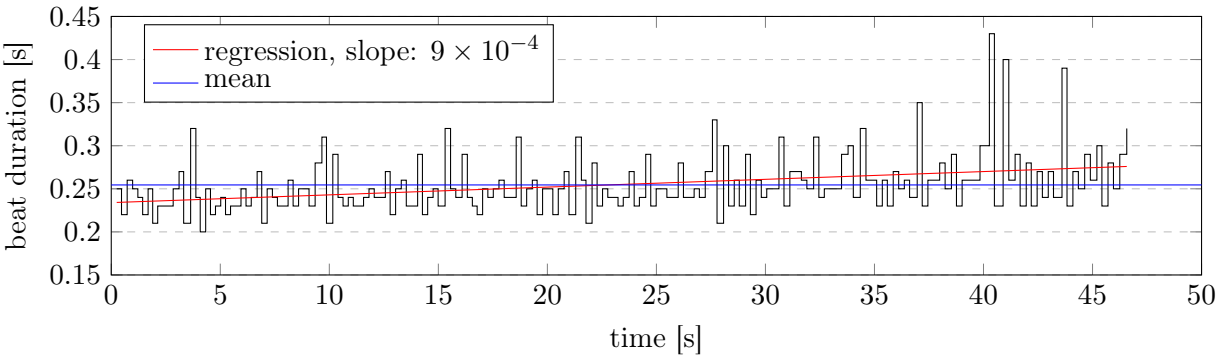

Figure 13: beat duration at the empirical profile wheel

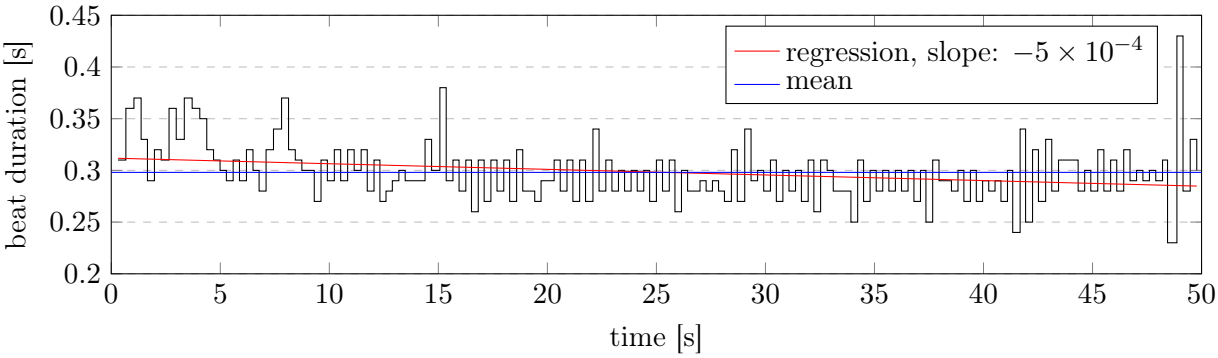

Figure 14: beat duration at the calculated profile wheel

Figure 13 and Figure 14 show the time course of the beat durations together with their linear regression as an overall trend: While the empirical profile wheel shows a positive increase in the average beat duration, that of the calculated profile wheel shows a negative slope. These overall tendencies of the beat durations can be justified with the hypotheses presented above, according to which the empirical profile wheel forces a higher frequency with high spring force, whereas the calculated profile wheel with high spring force initially provides higher friction and thus slows down the balance wheel.

The diagrams also show that the calculated profile wheel, lasting 49.78 s, runs longer at a stretch than the empirically determined one, which maintains the balance oscillation for 46.57 s; however, this is mainly due to the higher oscillation frequency; with 184 beats compared to 168, the empirically determined profile wheel transfers more energy to the balance wheel over the entire running time[16]. Another indication of the calculated profile wheel's higher performance is the slope value of the regression line: Since $|-5 \times 10^{-4}| < |9 \times 10^{-4}|$, the average period is less of dependent on time, so that I see my hopes of the curve calculation regarding higher accuracy fulfilled. So the calculated profile wheel appears to have better accuracy at the cost of slightly less force tolerance or "reliability", in contrast to the empirical profile wheel, which runs rather erratically but over a greater range of forces.

The time interval between 20 s and 25 s exhibits even more interesting behaviour of the calculated profile wheel's beat duration, as the continuously alternating beat durations – as expected – are clearly visible. From this it can be concluded that the profile wheel is not attached in a neutral position. If one counts the beats up to the corresponding digits, one comes to the conclusion

[16] Because during each beat, the mainspring relaxes further by a fixed angle and the more the spring has relaxed, the more energy it has transferred.

that the beat consisting of the first blocking phase and the second drive phase[17] takes longer than the other. If one assumes – as before – that the longer duration is caused by a longer acceleration path of the balance wheel, it can be reasoned that the profile wheel in Figure 5 is twisted clockwise relative to the non-deflected orientation.
Finally, I would like to point out that the systematically alternating beat durations in the empirical profile wheel hardly appear in the series of measurements, because the beat durations change continuously without exhibiting the previously described pattern of alternating durations; only irregular fluctuations can be seen in the diagram. This is another aspect that shows that the calculated profile wheel causes the clockwork's rate to be more regular.

[17]The clicking is emitted from the escapement at the beginning of the second blocking phase (Figure 5d) .